18th International Conference on Information Fusion
Washington, DC - July 6-9, 2015

TRACK BEFORE DETECT DOA TRACKING OF EXTENDED TARGETS WITH MARKED POISSON POINT PROCESSES

Augustin-Alexandru Saucan[†] *Thierry Chonavel*[†] *Christophe Sintes*[†] *Jean-Marc Le Caillec*[†]

{augustin.saucan, thierry.chonavel, christophe.sintes, jm.lecaillec}@telecom-bretagne.eu
[†] Institut Mines Telecom - Telecom Bretagne, CNRS UMR 6285 LabSTICC,
Technopôle Brest-Iroise - CS 83818 - 29238 Brest Cedex 3 - France

ABSTRACT

In this paper we propose a novel Track Before Detect (TBD) filter aimed at tracking multiple extended targets from phased-array observations. For extended targets, the source signal is angularly distributed, and hence we track the centroid Direction Of Arrival (DOA) of the target generated signal - called target signal. In this work we suppose known the shape and extent of the target-signal angular spread. Solutions based on extending the system state, to include the target signal, lead to higher-dimensional posteriors. We avoid an extended state by using a novel Marked Poisson Point Process (MPPP) model for the system, and accordingly, we derive the intensity/PHD filter that adaptively estimates target number and corresponding centroid DOAs. The source signals are interpreted as the mark of a target, and they are analytically integrated in the update formula of the filter. Therefore, an efficient particle filter implementation is possible. Results on simulated data showcase the improved results of the proposed filter over state-of-the-art methods.

Index Terms**—** DOA tracking, marked Poisson point process, track before detect, extended target, DBSCAN.

I. INTRODUCTION AND RELATED WORK

The work presented in this paper focuses on tracking of acoustic waves in underwater environments with phased-array sonar antennas, comprising of vertically-stacked hydrophone arrays. Examples of applications include tracking of kinematic targets [1] such as submarines, torpedoes; or sea-floor image reconstruction [2] by means of adaptively filtering echoes backscattered by the sea-bottom or some object of interest. Our proposed filter is general, and can be employed for either kinematic target tracking or adaptive echo filtering for imaging applications. 3-D sea-bottom reconstruction, called bathymetry, involves the localization of extended targets - resolution cells projected onto the sea-bottom. In all phased-array based applications, target localization is synonymous with estimating the DOA of the echo backscattered by the specific target. Shallow waters constitute a difficult environment, exhibiting persistent clutter due to the multi-path propagation between the two boundaries: sea-bottom and sea-surface. In such environments, classical array processing methods lead to spurious DOA estimates due to dense and persistent clutter [3]. In [4], [2] and [5] we employed tracking methods to separate the DOA trajectory of the "informative" echoes, that is, the direct line-of-sight echoes, from "interfering" higher-order echoes. In [5] and [2] we proposed a Track While Scan (TWS) approach, where DOA observations were inferred from the signal spectrogram and subsequently filtered with Probability Data Association (PDA) algorithms [6].

Track Before Detect (TBD) filters track targets directly from the phased-array signal, without the need of pre-detection or pre-estimation procedures. Any detection procedure is effectively delayed until after the tracking phase [1, Ch. 7.8], conferring the ability to track low Signal to Noise Ratio (SNR), or dim targets. In [4] we proposed a TBD filter capable of tracking up to two simultaneous echoes by using a multiple model framework. In order to cope with a generic number of targets we employ a PPP to model target locations [7]. Practical filters propagating only the first-order moment measure density of the PPP multi-target process, referred to as the intensity or the Probability Hypothesis Density (PHD) [8] function, have been proposed in [9] and in [10]. However, both the intensity filter and the PHD filter are derived for TWS systems and are not directly applicable to TBD. A first PHD-TBD filter was proposed in [11] using a Multi-Bernoulli prior, for a specific case of separable likelihood observations. In contrast, for array signals this is not verified and the observation model is deemed *superpositional* [12]. Namely, the observed array signal is a sum of individual target generated signals - the target signals. For superpositional amplitude sensors a PHD-TBD filter was proposed in [12]. However, for phased-arrays the DOA information is contained in the phase differences between the signals received by the sensor array and, in general, we are not directly interested in signal amplitudes. Furthermore, signal amplitudes are random variables, with the method in [12] not being directly applicable. A possible work-around solution would be to augment the state of each target with the source signal. However, for particle filter implementations, sampling from higher dimensional posteriors is inefficient. Such a solution is undertaken in [13], coupled with a reversible jump MCMC algorithm to handle fluctuations in target number. In [14] the authors propose a multi-Bernoulli filter coupled with the MUSIC [15, Ch. 4.5] pseudo-spectrogram in order to track several targets from array observations. In [16], the minimum mean optimal sub-pattern assignment estimator is employed to resolve closely spaced point targets. While in [17], a fuse-before-track approach is undertaken, to fuse the raw signals obtained from different acoustic sensors and extract target trajectories form the fused result.

The novelty of our approach is the proposal of an extended target Marked PPP model, and the derivation of the intensity filter for extended target DOA tracking. Thus, we extend in the case of MPPP the aforementioned multi-target TBD filters and we extend our work in [18], which considered only point targets. The MPPP formalism naturally describes targets that generate a *mark*, here a stochastic signal characterizing the individual extended-target contribution. The mark distribution we propose, takes into account the extended target model. The observations of our filter are the noisy superposition of individual target marks. The propagation of the PPP intensity function is shown to be sufficient, leading to a more efficient particle filter implementation than filters propagating extended states defined on the augmented space of target location and mark spaces. We highlight the ability of the proposed filter to deliver target DOA estimates for each array observation. This is a vital requirement for high-resolution image formation algorithms, e.g. sonar bathymetry reconstruction [4]. In contrast, the method of [14] and most TWS methods [5] process a small block of array observations in order to produce a single DOA estimate. Thus, generally resulting in an overall reduced resolution image.

The paper is organized as follows: section II presents the extended target signal model and the MPPP array observation formalism. In section III we derive the approximate intensity filtering equations. In section IV we showcase results on simulated data of our proposed filter and we conclude in section V.

II. PHASED-ARRAY SIGNAL AND MPPP FORMALISM

Throughout this paper, point processes (PP) are employed to model a random number of targets characterized by random (location) state vectors. We consider at time t the random process X_t to represent a finite and simple PP with realizations of the form $\mathsf{x}_t = \{\mathbf{x}_{1,t}, \dots, \mathbf{x}_{n_t,t}\}$. Where both the number of targets n_t and target states $\mathbf{x}_{i,t}$ are random. Each target state vector takes values in the single-target space: $\mathbf{x} \in \mathcal{R}$, usually some subspace of $\mathbb{R}^d$ and evolves in time according to the state equation

$$\mathbf{x}_t = F_t\,\mathbf{x}_{t-1} + \mathbf{v}_t, \tag{1}$$

where F_t is the transition matrix and $\mathbf{v}_t$ is the model noise supposed a zero mean, white Gaussian process with covariance matrix Q_t, i.e. $\mathbf{v}_t \sim \mathcal{N}(\mathbf{v}; \mathbf{0}, Q_t)$. Array observations consist in a noisy sum of individual target contributions, i.e. target signals, which are also treated as random variables. The statistics of target contributions and array observation are treated in section II-A. The marked point process that describes target number, location and target generated signals is presented in section II-B.

II-A. Extended target model

Considering the multi-target PP X_t, with the vector $\mathbf{x}_{i,t}$ representing the state of the i-th extended target, the $M-$element array observation signal $\mathbf{y}_t \in \mathcal{Y}$, with $\mathcal{Y} \subset \mathbb{C}^{M\times 1}$, is

$$\mathbf{y}_t = \sum_{i=1}^{n_t} \mathbf{s}(\mathbf{x}_{i,t}) + \mathbf{w}_t, \tag{2}$$

where $\mathbf{s}(\mathbf{x}_{i,t})$ is the contribution of the i-th extended target, referred to as target or source signal. The additive observation noise $\mathbf{w}_t \in \mathbb{C}^{M\times 1}$ is taken to be Gaussian with parameters: $\mathbf{w}_t \sim \mathcal{N}(\mathbf{n}; \mathbf{0}, \sigma^2 I_M)$.

Each extended target emits a signal $\mathbf{s}(\mathbf{x}_{i,t})$ dependent on the target state, and which in point process terminology represents a mark. Given the nature of extended targets, the mark [19] is given by

$$\mathbf{s}(\mathbf{x}_{i,t}) = \int_{-\pi}^{\pi} \mathbf{a}(\phi)\,\mathcal{S}(\phi; \mathbf{x}_{i,t}) d\phi, \tag{3}$$

which explicitly models the extended target signal as the sum of backscattered signals $\mathcal{S}(\phi; \mathbf{x}_{i,t})$ of elementary scatterers having the DOA ϕ. Eq. (3) is specific to targets having an angular spread and for linear arrays, motivating the integration interval of $[-\pi, \pi]$. Furthermore, each elementary backscattered signal is treated as a narrow-band plane wave with DOA ϕ and array manifold vector $\mathbf{a}(\phi)$. A typical form of $\mathbf{a}(\cdot)$ for linear and uniformly spaced arrays is defined as

$$\mathbf{a}(\phi) \triangleq \begin{bmatrix} 1 & e^{-j\,\phi} & \cdots & e^{-j\,(M-1)\phi} \end{bmatrix}^T,$$

where $\{\cdot\}^T$ represents the transpose operator. The DOA ϕ is linked to the physical angle θ by: $\phi = k\Delta\sin(\theta)$, where k represents the wave number, M the number of hydrophones in the array and Δ the hydrophone spacing. Note that the physical angle spans $\theta \in [-\pi/2, \pi/2]$ for linear arrays.

Whenever scattering from rough surfaces is involved [20], [19], the process $\mathcal{S}(\cdot)$ is considered white, that is

$$E\{\mathcal{S}(\phi; \mathbf{x}_{i,t})\mathcal{S}(\phi'; \mathbf{x}_{i,t})\} = P(\mathbf{x}_{i,t})\rho(\phi; \mathbf{x}_{i,t})\delta(\phi - \phi')$$

where $\delta(\cdot)$ is the Dirac impulse and $E\{\cdot\}$ is the expectation operator. $P(\mathbf{x}_{i,t})$ is the average power of the target having state $\mathbf{x}_{i,t}$ with $\rho(\phi; \mathbf{x}_{i,t})$ generating the specific shape of the angular spread of the target's power in the observation angle of 2π. The form of the angular distribution of power $\rho(\cdot)$ influences the shape of the covariance matrix of the array received signal. Examples for $\rho(\cdot)$ are given in [21], and in general have two main parameters: the mean $\bar{\phi}(\mathbf{x}_{i,t})$ and variance σ_ϕ^2. In this work we consider the Gaussian $\rho(\cdot)$ of [21, Sec. 2.2]:

$$\rho(\phi;\mathbf{x}_{i,t}) = \frac{1}{\sqrt{2\pi\sigma_\phi^2}}\exp\left(-\frac{(\phi-\bar{\phi}(\mathbf{x}_{i,t}))^2}{2\sigma_\phi^2}\right). \quad (4)$$

where $\sigma_\phi \ll \pi$ is the, supposedly known, angular spread of $\rho(\cdot)$. Note that $\rho(\cdot)$ is a true distribution, i.e. $\rho(\phi) \geq 0$ for any $\phi \in [-\pi, \pi]$ and $\int \rho(\phi)d\phi = 1$.

The elementary backscattered signals $\mathcal{S}(\cdot)$ are considered a Gaussian process indexed by ϕ, with parameters $\mathcal{S}(\phi;\mathbf{x}_{i,t}) \sim \mathcal{N}(\mathcal{S};0,P(\mathbf{x}_{i,t})\rho(\phi;\mathbf{x}_{i,t}))$. This ensures a Gaussian distributed mark

$$\mathbf{s}(\mathbf{x}_{i,t}) \sim \mathcal{N}(\mathbf{s};0,R_{i,t}), \quad (5a)$$

$$[R_{i,t}]_{m,n} = P(\mathbf{x}_{i,t})e^{-\frac{(n-m)^2\sigma_\phi^2}{2}}e^{j(n-m)\bar{\phi}(\mathbf{x}_{i,t})}, \quad (5b)$$

where the specific form of the mark covaraince matrix is given by the shape of the angular power distribution $\rho(\cdot)$ of eq. (4). The array observation likelihood, given the multi-target PP and associated marks is

$$\mathbf{y}_t|(\mathbf{x}_{i,t},\mathbf{s}(\mathbf{x}_{i,t}))_{i=1,\dots,n_t} \sim \mathcal{N}(\mathbf{y};\sum_{i=1}^{n_t}\mathbf{s}(\mathbf{x}_{i,t}),\sigma^2 I_M). \quad (6)$$

In relationship to the noise variance σ^2, the Signal to Noise Ratio (SNR) of the i-th target is given by $SNR = P(\mathbf{x}_{i,t})/\sigma_t^2$. In the following section, the multi-target state and target mark distributions is captured in a unitary framework using marked point processes.

II-B. MPPP formalism

The most widely employed class of PP in target tracking is the Poisson PP (PPP) [8], [9]. A PPP exhibits a Poisson distribution for the number of targets n_t with mean $\int_\mathcal{R}\lambda_t(\mathbf{x})d\mathbf{x}$ and iid target states with probability density $\lambda(\mathbf{x})/\int_\mathcal{R}\lambda_t(\mathbf{x})d\mathbf{x}$. A compact representation for PPPs is achieved via the Janossy density [22, Ch. 5.3]:

$$p(\mathsf{X}_t) = e^{-\int_\mathcal{R}\lambda_t(\mathbf{x})d\mathbf{x}}\prod_{\mathbf{x}\in\mathsf{X}_t}\lambda_t(\mathbf{x}). \quad (7)$$

For PPPs, observe that both number and point locations are completely characterized by the intensity function $\lambda_t(\cdot)$. Furthermore the first-order moment measure density for PPP equals the intensity function [23, Sec. 3.4] and is also referred to as the PHD [8]. As noted in [22, Ch. 5.4, p. 136], the quantity $\lambda_t(\mathbf{x})d\mathbf{x}$ represents the probability of finding one target in $[\mathbf{x},\mathbf{x}+d\mathbf{x})$, with the interpretation that peaks of $\lambda_t(\cdot)$ determine target locations while it's integral over a specific region yields the average number of points belonging to that region.

In order to accommodate both target locations and target generated signals, we introduce the Marked PPP $\tilde{\mathsf{X}}_t$ with realizations of the form $\tilde{\mathrm{x}}_t = \{(\mathbf{x}_{i,t},\mathbf{s}(\mathbf{x}_{i,t}))|i=1,\dots,n\}$ containing the pairs of target state and target mark (target signal). The PPP X_t describing only target number and position is usually denoted as ground PPP [22, Ch. 6.4]. The MPPP has the same cardinality of the ground PPP, hence it is also a Poisson PP with intensity function given by the Marking Theorem [24, Prop. 3.9] and [25, p. 55]: $\tilde{\lambda}_t(\tilde{\mathbf{x}}) = \lambda_t(\mathbf{x})\mathcal{N}(\mathbf{s};\mathbf{0},R(\mathbf{x}))$, with $\tilde{\mathbf{x}}$ denoting the pair $(\mathbf{x},\mathbf{s}(\mathbf{x}))$ and $R(\mathbf{x})$ given by eq. (5b).

In order to infer target positions from the MPPP $\tilde{\mathsf{X}}_t$, the knowledge of $\lambda_t(\mathbf{x})$ is sufficient. The number of targets in any region $\mathcal{A} \in \mathcal{R}$ is given by $\int_\mathcal{A}\lambda_t(\mathbf{x})d\mathbf{x}$. Target centroid DOAs can be obtained from the locations of the main peaks of $\lambda_t(\cdot)$. The aim of the proposed filter is to adaptively detect targets and estimate target states $\mathbf{x}_t$ from the MPPP posterior process $\tilde{\mathsf{X}}_t|\mathbf{y}_{0:t}$, given the sequence $\mathbf{y}_{0:t}$ of past and current array observations. In order to achieve this goal, propagation of the corresponding PPP intensity $\lambda_{t|t}(\mathbf{x})$ is sufficient while the MPPP intensity $\tilde{\lambda}_{t|t}(\mathbf{x})$ occurs naturally in the observation likelihood. In such, the propagation of $\lambda_{t|t}(\mathbf{x})$ is conducted in the state-space $\mathcal{R}$, avoiding the propagation in the augmented space $\mathcal{R}\times\mathbb{C}$ [13]. Approximate propagation formulas for $\lambda_{t|t}(\mathbf{x})$ are derived in the following section.

III. MPPP INTENSITY FILTER

In this section, we derive the filtering equations for tracking extended targets via phased-array observations. We aim at deriving the intensity $\lambda_{t+1|t+1}(\mathbf{x})$ corresponding to the posterior ground PPP given past and current array observations. The filter comprises two stages: prediction (sec. III-A) and update (sec. III-B). In the prediction stage, we derive an exact formula for $\lambda_{t+1|t}(\mathbf{x})$. We take into account target kinematics as dictated by the law of motion of eq. (1), and target death and birth. The update stage intends to correct the predicted intensity with the current observation $\mathbf{y}_{t+1}$. Closed form formulas are not available for the updated intensity, and an approximation similar to [12] is proposed.

III-A. MPPP intensity Prediction

Consider at time t the intensity $\lambda_{t|t}(\cdot)$ corresponding to the posterior PPP $\mathsf{X}_{t|t} \triangleq \mathsf{X}_t|\mathbf{y}_{0:t}$. The PPP describing target locations at time t undergoes a stochastic transformation induced by target death and movement of the surviving targets. Since both the process at time t and the prediction process are PPPs, the prediction operation is exact and $\lambda_{t+1|t}$ is a sufficient statistic for the prediction PPP process.

Trajectory termination, or target death is modeled by a process of independent (Bernoulli) thinning. That is, targets present at time t survive with probability $p_s(\mathbf{x})$. The survival of targets is independent of each other. The resulting process is a PPP with intensity $p_s(\mathbf{x})\lambda_{t|t}(\mathbf{x})$ [24, Prop. 3.7]. Each point of the thinned PPP undergoes a kinematic transformation as dictated by the transition density $f_{t+1|t}(\mathbf{x}|\xi) = \mathcal{N}(\mathbf{x};F_{t+1}\xi,Q_t)$ of the kinematic model in eq. (1). The resulting process is again a PPP [7, Ch. 2.11.1]. Furthermore, to account for target birth, an independent PPP with intensity $\gamma_{t+1}(\cdot)$ is superposed to the transformed PPP. In virtue of the Superposition Theorem [25, Ch. 2.2], the predicted intensity is given by

$$\lambda_{t+1|t}(\mathbf{x}) = \gamma_{t+1}(\mathbf{x}) + \int_{\mathcal{R}} f_{t+1|t}(\mathbf{x}|\xi)\, p_s(\xi)\, \lambda_{t|t}(\xi) d\xi. \quad (8)$$

The predicted intensity captures target death, birth and kinematics. In the case of the MPPP, the predicted intensity is given by

$$\tilde{\lambda}_{t+1|t}(\tilde{\mathbf{x}}) = \lambda_{t+1|t}(\mathbf{x}) \mathcal{N}(\mathbf{s}; 0, R(\mathbf{x})) \quad (9)$$

As shown in the following section, the propagation of $\lambda_{t|t}(\mathbf{x})$ is sufficient, with the MPPP intensity intervening in the array likelihood model. This leads to an efficient implementation propagating only a particle approximation of $\lambda_{t|t}(\mathbf{x})$.

III-B. MPPP intensity Update

The updated intensity (PHD) $\lambda_{t+1|t+1}(\cdot)$ is obtained by means of marginalizing the posterior density [22, Lemma 5.4.III],

$$\lambda_{t+1|t+1}(\mathbf{x}) = \sum_{n=0}^{\infty} \frac{1}{n!} \int \cdots \int p_{t+1|t+1}(\{\mathbf{x}, \mathbf{w}_1, \ldots, \mathbf{w}_n\}) d\mathbf{w}_1 \cdots d\mathbf{w}_n.$$

Or more compactly, by using the set integral representation of [8, eq. 21]

$$\lambda_{t+1|t+1}(\mathbf{x}) = \int p_{t+1|t+1}(\{\mathbf{x}\} \cup \mathsf{W}) \delta \mathsf{W}$$

where $\mathsf{W} = \{\mathbf{w}_1, \cdots, \mathbf{w}_n\}$ has the same distribution as $\mathsf{X}_{t+1|t}$. Applying the Bayes rule for the posterior $p_{t+1|t+1}(\mathsf{W})$, and considering a Poisson expression (eq. (7)) for $p_{t+1|t}(\mathsf{W})$ we obtain [12]:

$$\lambda_{t+1|t+1}(\mathbf{x}) = \lambda_{t+1|t}(\mathbf{x})\, L_{t+1}(\mathbf{x}). \quad (10)$$

The ratio $L_{t+1}(\mathbf{x})$ is given by:

$$L_{t+1}(\mathbf{x}) = \frac{\int p_{t+1}(\mathbf{y}_{t+1}|\{\mathbf{x}\} \cup \mathsf{W}) p_{t+1|t}(\mathsf{W}) \delta \mathsf{W}}{\int p_{t+1}(\mathbf{y}_{t+1}|\mathsf{W}) p_{t+1|t}(\mathsf{W}) \delta \mathsf{W}}. \quad (11)$$

Marginalizing in relationship to the target marks (5a), the array likelihood becomes

$$p_{t+1}(\mathbf{y}_{t+1}|\mathsf{W}) = \int \cdots \int p_{t+1}(\mathbf{y}_{t+1}|\tilde{\mathsf{W}}) \prod_{i=1}^{|\tilde{\mathsf{W}}|} \mathcal{N}(\mathbf{s}; \mathbf{0}, R(\mathbf{w}_i)) d\mathbf{s}(\mathbf{w}_i), \quad (12)$$

where $\tilde{\mathsf{W}}$ is the MPPP constructed from the ground PPP W. Both the ground and marked PPP have the same cardinal, denoted by $|\tilde{\mathsf{W}}|$. By employing this specific form for the array likelihood, coupled with the expression of $p_{t+1|t}(\mathsf{W})$ of eq. (7), and grouping of terms we obtain

$$L_{t+1}(\mathbf{x}) = \frac{\iint p_{t+1}(\mathbf{y}_{t+1} - \mathbf{s}(\mathbf{x})|\widetilde{W}) \mathcal{N}(\mathbf{s}; 0, R(\mathbf{x})) p_{t+1|t}(\widetilde{W}) \delta \widetilde{W} ds}{\int p_{t+1}(\mathbf{y}_{t+1}|\widetilde{W}) p_{t+1|t}(\widetilde{W}) \delta \widetilde{W}} \quad (13)$$

Note that we interchanged the integration order in the numerator of (13), since the integrated functions are non-negative.

By employing the change of variables formula proposed in [26, Prop 4., p.180], that is, denoting $\mathbf{z} \triangleq \sum_{\tilde{\mathbf{w}} \in \tilde{W}} \mathbf{s}(\tilde{\mathbf{w}})$, the denominator of (13) becomes:

$$\int p_{t+1}(\mathbf{y}_{t+1}|\widetilde{\mathsf{W}}) p_{t+1|t}(\widetilde{\mathsf{W}}) \delta \widetilde{\mathsf{W}} = \int \mathcal{N}(\mathbf{y}_{t+1}; \mathbf{z}, \sigma_t^2 I_M) p(\mathbf{z}) d\mathbf{z}. \quad (14)$$

Observe that in eq. (14) the set integrals are now reduced to ordinary integrals, where $p(\mathbf{z})$ is the distribution induced by the change of variables. As proposed in [12] if we approximate $p(\mathbf{z}) \approx \mathcal{N}(\mathbf{z}, \widetilde{\mu}, \widetilde{\Sigma})$ with a Gaussian distribution we are able to obtain an analytic formula for the updated intensity. The first and second order moments of $p(\mathbf{z})$ are obtainable from the MPPP predicted distribution $p_{t+1|t}(\widetilde{X})$ by means of the Marking Theorem [25, Ch. 5.3]:

$$\begin{aligned}\widetilde{\mu} &= \int \mathbf{s}(\widetilde{\mathbf{x}})\, \widetilde{\lambda}_{t+1|t}(\widetilde{\mathbf{x}}) d\widetilde{\mathbf{x}} \\ &= \iint \mathbf{s}(\mathbf{x})\, \lambda_{t+1|t}(\mathbf{x})\, \mathcal{N}(\mathbf{s}; 0, R(\mathbf{x})) d\mathbf{x} d\mathbf{s} = 0. \quad (15a)\\ \widetilde{\Sigma} &= \int \mathbf{s}(\widetilde{\mathbf{x}}) \mathbf{s}^H(\widetilde{\mathbf{x}})\, \widetilde{\lambda}_{t+1|t}(\widetilde{\mathbf{x}}) d\widetilde{\mathbf{x}} \\ &= \int R(\mathbf{x})\, \lambda_{t+1|t}(\mathbf{x}) d\mathbf{x}. \quad (15b)\end{aligned}$$

where $\widetilde{\lambda}_{t+1|t}(\widetilde{\mathbf{x}})$ is the predicted MPPP intensity given by eq. (9), and $\{\cdot\}^H$ represents the transpose conjugate operator. Under the approximation $p(\mathbf{z}) \approx \mathcal{N}(\mathbf{z}, \mathbf{0}, \widetilde{\Sigma})$ and using the formula for combination of quadratic terms [27, Appendix 3.8], we solve (14) and obtain

$$\int \mathcal{N}(\mathbf{y}_{t+1}; \mathbf{z}, \sigma_t^2 I_M) p(\mathbf{z}) d\mathbf{z} \approx \mathcal{N}(\mathbf{y}_{t+1}; \mathbf{0}, \sigma_t^2 I_M + \widetilde{\Sigma})$$

Solving in a similar manner the numerator of (13) we obtain

$$L_{t+1}(\mathbf{x}) \approx \frac{\mathcal{N}(\mathbf{y}_{t+1}; \mathbf{0}, R(\mathbf{x}) + \sigma_t^2 I_M + \widetilde{\Sigma})}{\mathcal{N}(\mathbf{y}_{t+1}; \mathbf{0}, \sigma_t^2 I_M + \widetilde{\Sigma})} \quad (16)$$

The updated intensity $\lambda_{t+1|t+1}(\cdot)$ follows from (10) where $L_{t+1}(\cdot)$ is approximated by (16).

IV. SIMULATION RESULTS

The predicted intensity (8) is updated with equation (10) were $L_{t+1}(\cdot)$ serves as a pseudo-likelihood function. Since the update equation is nonlinear in the state $\mathbf{x}$ (see the mark covariance of eq. (5b)), a sequential Monte Carlo method is employed for the implementation. Hence, the intensity function is approximately described by a set of weighted particles. This discrete point-mass approximation to the intensity function is propagated through the prediction and update steps with an auxiliary particle filter implementation, similarly to [12]. Since, we employ the approximation (16) in the update step, the integration of the intensity $\lambda_{t+1|t+1}(\cdot)$ over a region of $\mathcal{R}$ is no longer a reliable estimate for the average number of targets contained in that region. In such situations, clustering methods are employed to estimate the effective number of clusters and extract individual cluster centers from the particle cloud approximating $\lambda_{t+1|t+1}(\cdot)$. In [12] the authors propose to iterate the $k-$means clustering algorithm for different numbers of clusters. The decision regarding the number of clusters is selected in accordance with a "clustering quality" computed for each $k-$means iteration. This "clustering quality" is evaluated by measuring the separation of clusters with the silhouette method [28]. However, the silhouette method requires at least two clusters, and hence, cannot be applied to single target and void target situations, fact noted by the authors of [12]. We propose to use an improved clustering mechanism, relying on the DBSCAN method [29]. DBSCAN is a non-supervised clustering method, automatically detecting the number of clusters. Also, DBSCAN takes into account outliers, i.e. particles not belonging to any cluster. This is necessary since a number of particles created by the uniform-birth component of the intensity function, which do not belonging to any target are to be expected. The $k-$means algorithm behaves poorly in presence of outliers since it minimizes the sum of squared distances between particles belonging to the same cluster.

A test scenario involving three crossing extended targets was envisaged. We consider extended targets to be distributed with an angular distribution given by (4) and $\sigma_\phi = 0.1$ radians. The phased-array is a uniformly half-wavelength spaced array, composed of $M = 18$, while the extended targets are considered to emit target signals (or marks) of equal power $P(\mathbf{x})$ to assure an SNR of 5dB. Target kinematics assure a nearly constant speed model as given by (1). The target state $\mathbf{x}_t = [\theta_t, \dot{\theta}_t]^T$ is composed of the physical angle θ_t and the corresponding angular speed $\dot{\theta}_t$. Tracking targets directly in polar coordinates is possible when pseudo-accelerations are small [31, Ch. 1.5], a case we consider here. F_t is a transition matrix specific for a constant velocity model [32, Ch. 6.3.1]. The model noise is $\mathbf{v}_t \sim \mathcal{N}(\mathbf{v}; 0, Q_t)$ with covariance $Q_t = G q_t^2 G^T$ and acceleration $q_t = 0.3^o/s^2$. Accordingly, $G = \left[T_s^2/2,\, T_s\right]^T$ and $T_s = 1s$ represents the sampling period. The intensity filter parameters include a number of 1000 particles per target with the probability of target survival a constant of 0.9. The intensity, for birth location is taken to be uniform on the interval $[-\pi/2, \pi/2]$, i.e. $\gamma_t(\theta) \propto \mathbb{1}_{[-\pi/2,\pi/2]}(\theta)$. While for the speed of birth particles we use $\gamma_t(\dot{\theta}) \propto \mathcal{N}(\dot{\theta}; -2, 1)$. The whole birth intensity integrates to 0.2. Filtering results are shown in Figure 1-a) for the proposed MPPP intensity filter and in Figure 1-b) for a state-of-the-art TWS-PHD filter proposed in [30]. In both figures we show the true target tracks overlaid with the particle approximation of their respective estimated intensity functions. Furthermore, DBSCAN cluster centers are plotted for both methods. Parameters for DBSCAN are the minimum number of particles to form a cluster, set to 70, and the point neighborhood distance set to 3. We observe a better adequacy of the estimated intensity, and consequentially the clustering results, for the proposed method over the TWS method. Notably, the third

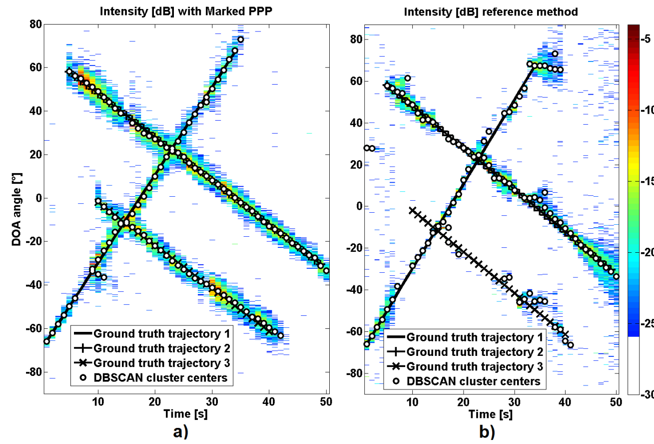

Fig. 1. True target tracks overlaid on the logarithm of the intensity function and DBSCAN clustering results for: a) proposed MPPP intensity filter b) TWS-PHD method of [30]

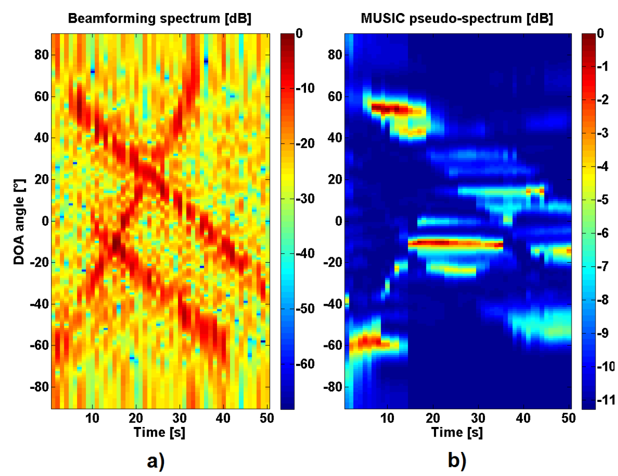

Fig. 2. Phased-array spectrograms: a) beamforming b) MUSIC.

Table I. Average OSPA error over 500 Monte Carlo runs.

	OSPA error for SNR $5dB$			OSPA error for SNR $0dB$		
Algorithm	$c = 1.5$	$c = 2.5$	$c = 5$	$c = 1.5$	$c = 2.5$	$c = 5$
Proposed PHD	0.81	0.94	1.14	0.89	1.05	1.26
Method in [30]	1.06	1.34	1.85	1.13	1.52	2.3

target birth is completely omitted by the TWS method. In order to better understand the behavior of the reference TWS method, we plotted the beamforming spectrogram and the MUSIC [33] pseudo-spectrogram in Figure 2-a) and b). The beamforming spectrogram is computed instantaneously, as $|TF(\mathbf{y}_t)|^2$, where $TF(\cdot)$ is the angular Fourier transform. The TWS method of [30] extracts the local maxima of the beamforming spectrogram in order to form the observation set. It is obvious from Figure 2-a) that such an observation set extraction method, leads to a high number of clutter points and the birth of the third target is buried in clutter and the large side-lobes of the first target. These side-lobes are specific for the beamforming method. Figure 2-b) showcases the MUSIC pseudo-spectrogram, which is computed on a sliding window of array observations $\mathbf{y}_t$. In order to compute a full-rank estimate of the array correlation matrix, the length of this window needs to be greater than the number of array receivers $M = 18$. Here we take the window to be of length 22, with the array covariance matrix obtained by averaging array observations within the supposed time window. In order to apply MUSIC, the number of targets is estimated with the Akaike information criterion [34]. As opposed to the instantaneous beamforming spectrogram, the MUSIC methods eliminates much of the spurious clutter but behaves poorly due to the highly non-stationary array signal. Indeed, the target angles appear to evolve too rapidly and the empirical array covariance matrix estimation leads to a smeared angle effect. This effect renders target DOA estimates irrecoverable from the MUSIC pseudo-sppectrogram. This illustrates the difficulty posed by scenarios with rapidly evolving targets in short time periods for classical array processing methods, like MUSIC.

A Monte Carlo analysis is conducted by simulating 500 times the same scenario described above at SNR values of 5dB and 0dB. The low SNR scenario of 0dB is conducted to test the proposed TBD intensity filter. The optimal subpattern assignment (OSPA) [35] error metric is employed to quantify the differences between the estimated target set and the ground truth set. The results are synthesized in Table I for order 2 and different cutoff c parameter values, showcasing again the superiority of the proposed TBD filter, even in very low SNR conditions.

V. CONCLUSIONS

Based on an MPPP formalism, a track before detect filter is proposed for tracking extended targets from phased-array observations. The extended target generated signals, modeled as the marks of the MPPP, are analytically integrated in the intensity update equation, ensuring a more efficient particle implementation of the intensity filter. Tracking of multiple crossing targets is considered, showcasing the improved performance of the proposed filter in comparison to TWS filters and classical array processing methods like MUSIC. Furthermore, a Monte Carlo simulation is performed depicting the robustness of our proposed method even at low SNR.

ACKNOWLEDGMENT

This work was funded by a grant from the *Direction Générale de l'Armement* (French MoD) and the Carnot Institute.

REFERENCES

[1] S. Blackman and R. Popoli, *Design and Analysis of Modern Tracking Systems*. Norwood, MA: Artech House, August 1999.

[2] A.-A. Saucan, C. Sintes, T. Chonavel, and J.-M. Le Caillec, "Model-based adaptive 3D sonar reconstruction in reverberating environments," *To appear in IEEE Transactions on Image Processing*, 2015.

[3] R. E. Hansen, H. J. Callow, T. O. Sæbø, and S. A. V. Synnes, "Challenges in seafloor imaging and mapping with synthetic aperture sonar," *IEEE Transactions on Geoscience and Remote Sensing*, vol. 49, no. 10, pp. 3677 – 3687, October 2011.

[4] A.-A. Saucan, C. Sintes, T. Chonavel, and J.-M. Le Caillec, "Robust, track before detect particle filter for bathymetric sonar application," in *Proceedings of the International Conference on Information Fusion*, 2014.

[5] A.-A. Saucan, T. Chonavel, C. Sintes, and J.-M. Le Caillec, "3-D bathymetric reconstruction in multi-path and reverberant underwater environments," in *Proceedings of the International Conference on Image Processing*, 2014.

[6] Y. Bar-Shalom, F. Daum, and J. Huang, "The probabilistic data association filter," *IEEE Control Systems Magazine*, vol. 29, no. 6, pp. 82–100, December 2009.

[7] R. L. Streit, *Poisson Point Processes*. New York: Springer-Verlag, 2010.

[8] R. Mahler, "Multitarget bayes filtering via first-order multitarget moments," *IEEE Transactions on Aerospace and Electronic Systems*, vol. 39, no. 4, pp. 1152 – 1178, October 2003.

[9] R. L. Streit and L. D. Stone, "Bayes derivation of multitarget intensity filters," in *Information Fusion, 2008 11th International Conference on*, June 2008, pp. 1–8.

[10] S. S. Singh, B.-N. Vo, A. Baddeley, and S. Zuyev, "Filters for spatial point processes," *SIAM Journal on Control and Optimization*, pp. 2275–2295, 2009.

[11] B.-N. Vo, B.-T. Vo, N.-T. Pham, and D. Suter, "Joint detection and estimation of multiple objects from image observations," *Signal Processing, IEEE Transactions on*, vol. 58, no. 10, pp. 5129–5141, Oct 2010.

[12] S. Nannuru, M. Coates, and R. Mahler, "Computationally-tractable approximate PHD and CPHD filters for superpositional sensors," *IEEE Journal of Selected Topics in Signal Processing*, vol. 7, no. 3, pp. 410 – 420, June 2013.

[13] J.-R. Larocque, J. P. Reilly, and W. Ng, "Particle filters for tracking an unknown number of sources," *IEEE Transactions on Signal Processing*, vol. 50, no. 12, pp. 2926 – 2937, December 2002.

[14] P. B. Choppala, P. D. Teal, and M. Frean, "Adapting the Multi-Bernoulli filter to phased array observations using MUSIC as pseudo-likelihood," in *Preceedings of the International Conference on Information Fusion*, 2014.

[15] P. Stoica and R. L. Moses, *Spectral Analysis of Signals*. Prentice Hall, 2005.

[16] M. Baum, P. Willett, and U. D. Hanebeck, "Mmospa-based direction-of-arrival estimation for planar antenna arrays," in *Sensor Array and Multichannel Signal Processing Workshop (SAM), 2014 IEEE 8th*, June 2014, pp. 209–212.

[17] C. Kreucher and B. Shapo, "A fuse-before-track approach to target state estimation using passive acoustic sensors," in *Information Fusion (FUSION), 2011 Proceedings of the 14th International Conference on*, July 2011, pp. 1–8.

[18] A.-A. Saucan, T. Chonavel, C. Sintes, and J.-M. Le Caillec, "Marked Poisson point process PHD filter for DOA tracking," in *To appear in the 23rd European Signal Processing Conference (EUSIPCO)*, Nice, France, Sept 2015.

[19] S. Shahbazpanah, S. Valaee, and A. Gershman, "A covariance fitting approach to parametric localization of multiple incoherently distributed sources," *Signal Processing, IEEE Transactions on*, vol. 52, no. 3, pp. 592–600, March 2004.

[20] P. Beckmann and A. Spizzichino, *The Scattering of Electromagnetic Waves from Rough Surfaces*. Norwood, MA.: Artech House, 1987. [Online]. Available: http://books.google.fr/books?id=QBEIAQAAIAAJ

[21] Y. Meng, P. Stoica, and K. Wong, "Estimation of the directions of arrival of spatially dispersed signals in array processing," *Radar, Sonar and Navigation, IEE Proceedings -*, vol. 143, no. 1, pp. 1–9, Feb 1996.

[22] D. J. Daley and D. Vere-Jones, *An Introduction to the Theory of Point Processes*. New York: Springer-Verlag, 2003, vol. I.

[23] R. L. Streit, "The probability generating functional for finite point processes, and its application to the comparison of PHD and intensity filters," *Journal of Advances on Information Fusion*, vol. 8, no. 2, pp. 119–132, December 2013.

[24] J. Møller and R. Waagepetersen, *Statistical Inference and Simulation for Spatial Point Processes*, ser. Chapman & Hall/CRC Monographs on Statistics & Applied Probability. CRC Press, 2004.

[25] J. Kingman, *Poisson Processes*. Oxford, UK: Clarendon Press, 1993.

[26] I. Goodman, R. Mahler, and H. Nguyen, *Mathematics of Data Fusion*. New York: Kluwer Academic Publishers, 1997.

[27] B. Ristic, S. Arulampalam, and N. Gordon, *Beyond the Kalman Filter*. Artech House, 2004.

[28] P. J. Rousseeuw, "Silhouettes: A graphical aid to the interpretation and validation of cluster analysis," *Journal of Computational and Applied Mathematics*, vol. 20, pp. 53 – 65, 1987.

[29] M. Ester, H. Kriegel, J. Sander, and X. Xu, "A density-based algorithm for discovering clusters in large spatial databases with noise," in *International Conference on Knowledge Discovery and Data Mining*, 1996.

[30] B. Balakumar, A. Sinha, T. Kirubarajan, and J. P. Reilly, "PHD filtering for tracking an unknown number of sources using an array of sensors," in *Proceedings of the 13th IEEE Workshop on Statistical Signal Processing*, 2005.

[31] E. Brookner, *Tracking and Kalman Filtering Made Easy*. New York: John Wiley and Sons, 1998.

[32] Y. Bar-Shalom, X. Rong Li, and T. Kirubarajan, *Estimation with Applications to Tracking and Navigation: Algorithms and Software for Information Extraction.* Hoboken, NJ: John Wiley and Sons, July 2001.

[33] R. O. Schmidt, "Multiple emitter location and signal parameter estimation," *IEEE Transactions on Antennas and Propagation*, vol. 34, no. 3, pp. 276–280, March 1986.

[34] M. Wax and T. Kailath, "Detection of signals by information theoretic criteria," *IEEE Transactions on Acoustics, Speech and Signal Processing*, vol. 33, no. 2, pp. 387 – 392, April 1985.

[35] D. Schuhmacher, B.-T. Vo, and B.-N. Vo, "A consistent metric for performance evaluation of multi-object filters," *IEEE Transactions on Signal Processing*, vol. 56, no. 8, pp. 3447–3457, August 2008.